Modeling Distance Nonlinearity in ToF Cameras and Correction Based on Integration Time Offsets

Claudio Uriarte[1], Bernd Scholz-Reiter[1], Sheshu Kalaparambathu Ramanandan[1,2], and Dieter Kraus[2]

[1] Bremer Institut für Produktion und Logistik, BIBA, Bremen, Germany
{uri,bsr,kaa}@biba.uni-bremen.de
[2] Institute of Water-Acoustics, Sonar-Engineering and Signal-Theory, University of Applied Sciences Bremen, Bremen, Germany
Dieter.Kraus@hs-bremen.de

Abstract. Time of Flight (ToF) cameras capture the depth images based on a new sensor technology allowing them to process the whole 3D scenario at once. These cameras deliver the intensity as well as the amplitude information. Due to difference in travel time of the rays reaching the sensor array, the captured distance information is affected by non linearities. In this paper, the authors propose three models (the monostatic, bistatic and optimized) for correcting the distance non linearity. The thermal characteristic of the sensor is studied in real time and analysis for integration time offsets for different reflectivity boards are carried out. The correction results are demonstrated for different reflectivity targets based on our models and analyzed integration offsets.

Keywords: Photonic-Mixer-Device, calibration, integration time, ToF camera, bistatic modeling, monostatic modeling.

1 Introduction

The PMD cameras work with the Time-of-Flight principle. A light source mounted on the camera emits modulated light that travels to the target. The reflected light travels back to the pixel array in the sensor, where it is correlated. The correlation result is a measure of the distance to the target. This distance measure is affected by non linearities due to different travel time of the rays. Ideally the travel time is approximated to be a constant in the measurement principle, but in practice this introduces distance non linearities in the captured image. Another major problem with the ToF cameras is that the amount of reflected light strongly depends on the reflectivity of the objects which leads to erroneous distance calculations. The exact reason is not discovered yet. A black target placed at the exactly the same distance to the camera as a white one shows differences in distance measurements dependent on integration time. In this paper, a method is proposed for correcting the distance non linearities as well as the integration time offsets for different reflectivity. Chapter 2 outlines the experimental setup used for the measurements. Chapter 3 outlines the thermal characteristics of the camera and chapter 4 presents the three models proposed by the authors. Chapter 5 outlines the real test results carried out for black

C. San Martin and S.-W. Kim (Eds.): CIARP 2011, LNCS 7042, pp. 214–222, 2011.

and white boards for various integration times. Chapter 6 presents the non linear as well as integration time offset correction results for a checkered board. Finally chapter 7 concludes this paper.

2 Experimental Setup

The setup consists on a CamCube 2.0 PMD camera from PMDTechnologies [1] mounted on a sled on a linear motion table allowing a perpendicular motion towards and away from a board on which the paper targets are fixed. The sled is driven by a stepper motor allowing a maximum travelling distance of 7800mm. The roll, pitch and yaw of the camera can be manually adjusted with the camera mount. To simplify the time-consuming measurements, the data acquisition was fully automated using a PC running Windows XP SP3. A Matlab script was used both to communicate with the motor controller as well as to acquire the data.

Fig. 1. Experimental setup with a computer controlled motion table

The measurements were done in the dark, with only the integrated LED-array as light source. To prevent the effects of unwanted reflection from objects near the setup, a zig-zag shader was built to cover the metal guide, as proposed by [2]. In the same manner a wall cardboard boxes was built along the side the linear motion table. All other exposed surfaces were covered with a low reflection black cloth. The experimental setup is shown in Figure 1.

For the characterization measurements only the center pixel (103,103) of the sensor was used and the camera was held perpendicular to the target. To adjust the pitch and yaw, the camera was placed at 1000mm from the board and several measurements of the target board were performed and averaged. The pixel having the shortest distance was identified and the rotation of the camera adjusted in that direction. This procedure was repeated several times for the pitch and yaw until the center pixel showed the shortest average distance to the target.

3 Warm-Up Drift of the CamCube 2.0

Thermal drift is a major issue with sensors, as it affects their measuring accuracy until the operating temperature is reached. PMD cameras face a similar problem. In this experiment the thermal drift was determined. For this, a white target was placed at 3000 mm from the camera. After turn on readings were taken continuously for 8 hours for different integration times (50ms, 25ms and 5ms). The warm-up curves for the different integration times can be seen in figure 2. During the initial minutes of operation an unsteady behavior is noticed and the measurements are stabilized after approximately 60 minutes. In order to avoid any deviation errors due to warm-up, all the experiments mentioned in this paper are taken after a safe 60 minutes capturing time. The statistics for the experiment is shown in Table 1.

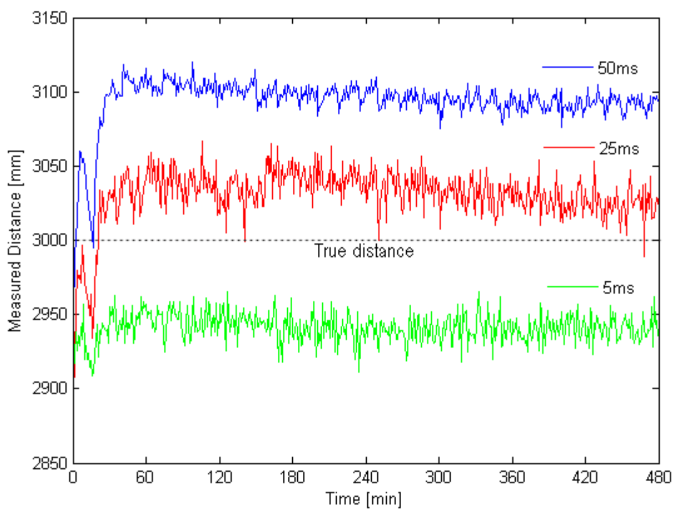

Fig. 2. Measured distances for a period of 8 hours of a white target placed at 3000mm

Table 1. Mean and standard deviation of the measurements of Figure 2

Integration time [ms]	Mean [mm]	Standard deviation [mm]
5	2941.4	6.6
25	3033.1	8.2
50	3096.7	4.8

4 Non Linear Distortion Modeling

Since the source and the receiver are spatially separated due to structural reasons, most of the ToF cameras exhibit a bistatic constellation. A preliminary investigation into such a constellation is outlined in [3]. The distance formula for any ToF Camera is given by:

$$D = c \cdot t_d / 2 \qquad (1)$$

(where D – distance between the camera and the observation point, c – speed of light and t_d – the time of flight of the transmitted signal). This equation is an approximation as t_d is assumed to be constant and hence is only valid for larger distances between the camera and the observation point. In practice, distance information for each pixel is altered according to the travel time of the rays impinging on it. The strength of the received signal is affected by the level of backscattering as well as the losses inside the medium. Some signal distortion models have been presented in [4] and [5]. The bistatic constellation modifies the travel time for different rays which introduces a nonlinear distance variation throughout the distance image. This distance variation can often be seen as a curvature when imaging objects perpendicular to the camera. If not accounted, this imaging non linearity can affect the whole system calibration procedure and can even affect all the post processing stages. In this paper a solution is presented by modeling the traversal paths by initially employing an ideal monostatic approach and then extending it to the practical scenario of bistatic constellation.

For our experiment, a plain perpendicular matted black board kept at 750 mm away is illuminated and imaged by the camera. The image formation is approximated to that of a pin hole camera model and the illustrations are shown in Figure 3.

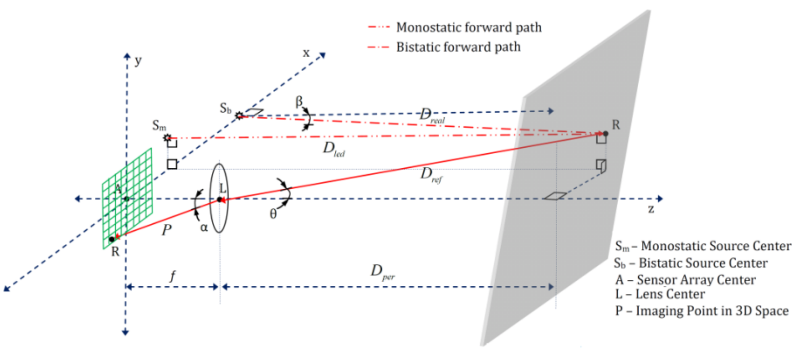

Fig. 3. Monostatic and bistatic models for distance correction

The distance measured by the PMD camera can be modeled as demonstrated in Figure 3. From the true monostatic model where the source and the receiver is at the same point, we introduce a small variation by assuming that the source is ideal rectangular and each imaging point on the 3D space is illuminated by a point source on x-y plane perpendicular to it. The light from the source hits the board at the point R, reflects back to the lens center at L and is focused on the sensor array. Ideally each light ray traverses a constant path length of D_{led}, variable path length of D_{ref} as well as a variable path length P according to the field of view of the camera (related to θ) and the focusing angle α. But practically D_{led} varies for each 3D point due to the spherical wavefront and interference. For the bistatic model, we assume that the source is kept at S_b imaging the point R in 3D space with the ray path length D_{real} making an angle β with the line parallel to z axis passing through S_b and perpendicular to x-y plane. Here the non linearities in the distance image are corrected by modeling the travel path of the reflected and transmitted rays. The correction required for each pixel is calculated by computing the true perpendicular distance D_{per} traversed by each ray from the board to the lens. All the following discussion includes the sensor to camera coordinates back projection [6] to find the angles θ, α and β given by the equations

$$x = f \cdot X_c / Z_c = (x_{im} - O_x) S_x \,. \tag{2}$$

$$y = f \cdot Y_c / Z_c = (y_{im} - O_y) S_y \,. \tag{3}$$

(where x, y – coordinates of sensor array; f – focal length ; X_c, Y_c – coordinates of the board; Z_c – distance from the camera to the board; O_x, O_y – principal point; x_{im}, y_{im} – image coordinates and S_x, S_y – size of the sensor pixel in both directions). Since the exact position of the board from the camera as well as the distance from the sensor array centre to the light source centre is known, the angles θ, α and β can be calculated geometrically. The CamCube 2.0 PMD camera has a focal length of 12.8mm and a pixel size of 40μm in both the sensor directions according to PMD Technologies [1]. Assuming that the indices (i,j,k) correspond to the coordinates of the imaged point R in 3D space, the measured distance D_{mes} can be rewritten from (1) as

$$D_{mes\,(i,j,k)} = (D_{led\,(i,j,k)} + D_{ref\,(i,j,k)} + P_{(i,j,k)}) / 2 \,. \tag{4}$$

From the mentioned monostatic model, the measured distance and the path length D_{led} can be approximated as

$$D_{mes\,(i,j,k)} = (D_{ref\,(i,j,k)} \cdot \cos(\theta_{(i,j,k)}) + f + D_{ref\,(i,j,k)} + P_{(i,j,k)}) / 2 \,. \tag{5}$$

$$D_{led\,(i,j,k)} = D_{ref\,(i,j,k)} \cdot \cos(\theta_{(i,j,k)}) + f \,. \tag{6}$$

The reflected ray is then given by (7). Hence the perpendicular distance to the lens from any imaged 3D point is given by (8) and thereby the corrected distance for monostatic model can be expressed as (9).

$$D_{ref\,(i,j,k)} = (2 \cdot D_{mes\,(i,j,k)} - f - P_{(i,j,k)}) / (1 + \cos(\theta_{(i,j,k)})) \,. \tag{7}$$

$$D_{per\,(i,j,k)} = D_{ref\,(i,j,k)} \cdot \cos(\theta_{(i,j,k)}) \,. \tag{8}$$

$$D_{cor(i,j,k)} = D_{per\,(i,j,k)} + f \,. \tag{9}$$

Modeling the bistatic constellation considering the angle β (from Figure 3), the reflected distance can be expressed similarly as

$$D_{ref\,(i,j,k)} = (2 \cdot D_{mes\,(i,j,k)} - (f / \cos(\beta_{(i,j,k)})) - P_{(i,j,k)}) / (1 + (\cos(\theta_{(i,j,k)}) / \cos(\beta_{(i,j,k)}))) \,. \tag{10}$$

The bistatic model uses this reflected distance to calculate the correction results from (8) and (9). Now an optimization method is presented for the previous monostatic model considering the path length of the reflected ray obtained from (7). The perpendicular distance to each 3D point calculated from (8) is used to find the optimized angular path traversed by the rays from the source to the board with the knowledge of β (from Figure 3). This optimized angular path can be given by

$$D_{opt\,(i,j,k)} = (D_{per\,(i,j,k)} + f) / \cos(\beta_{(i,j,k)}) \,. \tag{11}$$

The optimized path length is then applied in (4) to get the non linear correction from (7), (8) and (9). Results for the three approaches are presented in Figure 4 and 5.

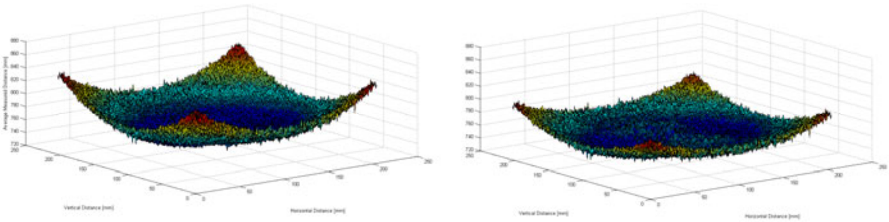

Fig. 4. Results of the measurement of a white target at 750mm from the camera; left: uncorrected distances; right: corrected distances using the monostatic model

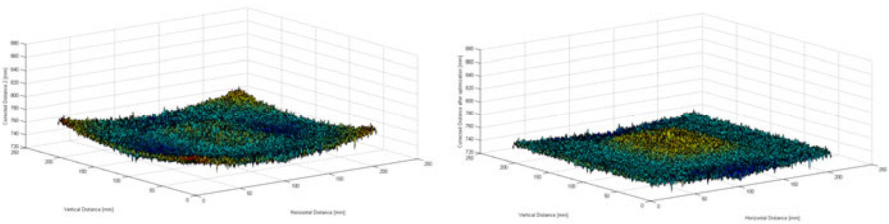

Fig. 5. Results of the measurement of a white target at 750mm from the camera; left: correction using the bistatic model; right: correction using the optimized model

5 Reflectivity Based Integration Time Offset Analysis

Preliminary results for distance correction based on the amplitude images have been published in [7]. Here, the problem is extended for a wide range of integration time. The experiment consists of imaging a black as well as a white board kept at true distances from 500 to 7000mm. The camera is moved in steps of 500mm. Each step measures the distance and amplitude for 16 different integration times varying from 1 to 46ms in steps of 3ms each. 500 samples of each integration time corresponding to a true distance are averaged to analyze the distance and amplitude variation for the centre pixel. The obtained 3D curve for measured distance and that for measured amplitude is plotted in Figures 6 and 7. A difference in amplitude as well as measured distance between the

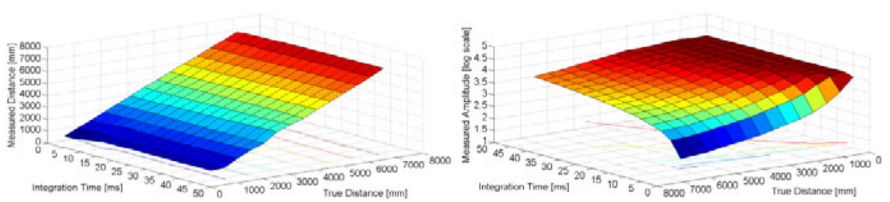

Fig. 6. Measured distance for different true distances and integration times for black target

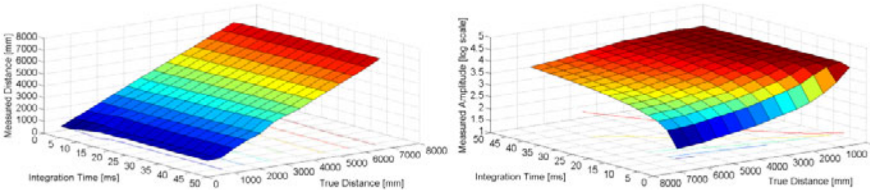

Fig. 7. Measured distance for different true distances and integration times for white target

black and white targets is observed and it is attributed to the differences in reflectivity. Distance and amplitude deviations due to different reflectivity are currently under research and preliminary results have been published in [8].

6 Combined Distance Correction

The black and white region can be clearly distinguished from the amplitude curves with respect to the integration time. Here an experimental demonstration is made for correcting a black and white checkered board based on both the prescribed non linear models as well as the integration time offsets. A multi dimensional LUT based approach is employed similar to [9] for distance offset correction. For the experiment, a black and white checkered board with a dimension of 420x297mm is mounted on the centre of an imaging board and is analyzed at a distance of 1000mm. The pattern consists of 5 black and 4 white checks arranged alternately. The integration time of the camera is set at 7ms. The distance images captured by the camera are back projected from (2) and (3) in Figure 8. The distance non linearities are corrected according to the bistatic and the optimization models presented in chapter 4.

A distance offset correction of 80mm is observed from the LUTs for the white board for the implemented integration time. The offset correction is done to the white checkered regions distinguished by the amplitude LUT. The final correction results are shown in Figure 9 and in Figure 10. Considerable improvements in the mean and standard deviation for a true distance of 1000mm were achieved (Table 2).

Table 2. Mean and standard deviation for the correction results for a true distance of 1000mm

Model	Mean [mm]	Standard deviation [mm]
Uncorrected	1046.6	27.5
Bistatic with Offset Correction	1008.7	9.7
Optimized with Offset Correction	996.5	9.5

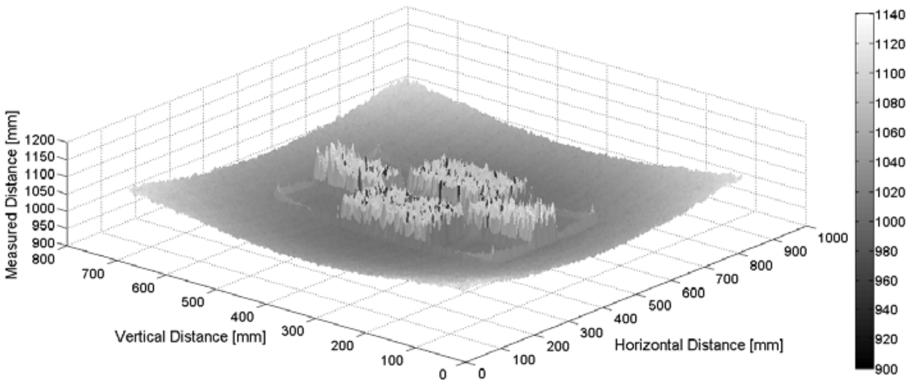

Fig. 8. Uncorrected distance measurement of a checkered target at a true distance of 1000mm

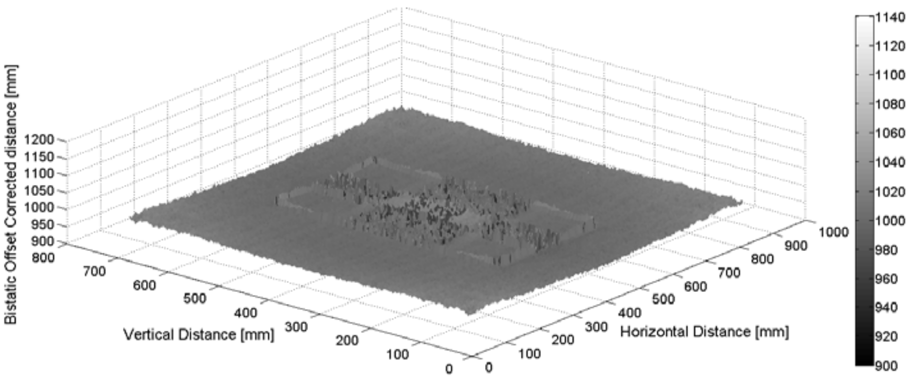

Fig. 9. Corrected distance using the bistatic model and distance offset

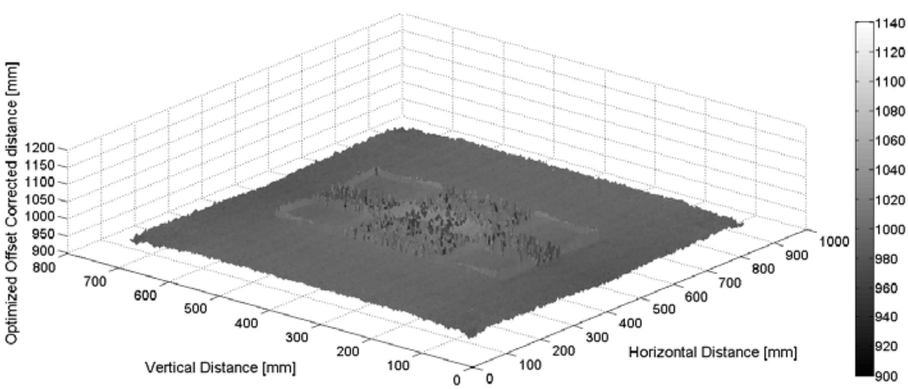

Fig. 10. Corrected distance using the optimized model and distance offset

7 Conclusion

In this paper the nonlinearities in the captured distance information of CamCube 2.0 is studied. Three models have been described in order to correct these non linear distance distortions. Characterization of the camera is performed and 60 minutes of warm up time is experimentally demonstrated. LUT based distance offset correction is demonstrated for different integration time and reflectivities. Finally the distance distortion in a black and white checkered pattern is corrected by combining the non linear distortion models as well as integration time offsets.

Further work will be done in the correction of the distance using a bistatic model considering the interference of the light sources of the camera. Sensor response to targets other than black and white will be determined in order to improve the calibration method.

Acknowledgement. The authors gratefully acknowledge the financial support by German Federal Ministry of Economics and Technology (BMWi) for the ROBOCON project.

References

1. PMD Technologies GmbH, `http://www.pmdtec.com/`
2. Rapp, H.: Experimental and Theoretical Investigation of Correlating TOF-Camera Systems. Diploma Thesis, University of Heidelberg, Heidelberg (2007)
3. Peters, V., Loffeld, O.: A Bistatic Simulation Approach for a High Resolution 3D PMD-Camera'. International Journal of Intelligent Systems Technologies and Applications 5(3/4) (2008)
4. Jamtsho, S., Lichti, D.: Modelling Scattering Distortion in 3D Range Camera. International Archives of Photogrammetry, Remote Sensing and Spatial Information Sciences, Newcastle, vol. XXXVIII (2010)
5. Mure-Dubois, J., Hugli, H.: Optimized Scattering Compensation for Time-of-Flight Camera. In: Proceedings of the SPIE Three-Dimensional Methodes for Inspection and Metrology V, Boston, vol. 6762 (2007)
6. Zhang, Z.: A Flexible New Technique for Camera Calibration. IEEE Transactions on Pattern Analysis and Machine Intelligence 22 (2000)
7. Oprisescu, S., Falie, D., Ciuc, M., Buzuloiu, V.: Measurements with ToF Cameras and their necessary corrections. In: Proceedings of the IEEE International Symposium on Signals, Circuits & Systems (ISSCS), Iasi, vol. 1, pp. 221–224 (2007)
8. Lindner, M., Schiller, I., Kolb, A., Koch, R.: Time-of-Flight sensor calibration for accurate range sensing. Computer Vision and Image Understanding 114(12), 1318–1328 (2010)
9. Kahlmann, T., Ingensand, H.: Calibration and Development for Increased Accuracy of 3D Range Imaging Cameras. In: Proceedings of the ISPRS Com., Dresden (2006)